Journal of Metals, Materials and Minerals, 34(2), 1979, 2024

Biosynthesis of zinc oxide nanoparticles using water hyacinth extracts: Characterization, evaluation of antimicrobial and dye removal

Phiphat SONTHONGPHITHAK[1], Chonchanok MUANGNAPOH[2], Chalita RATANATAWANATE[3], Teerasak E-KOBON[4], Akkharadet PIYASAENGTHONG[5], Piyorot HONGSACHART[6], Manop SRIUTTHA[6], Nipaporn SENGKHAMPARN[6], Anto Cordelia Tanislaus Anthony DHANAPAL[7], and Kitiyaporn WITTAYANARAKUL[6,*]

[1] *Program in Applied Bioresource Science, Faculty of Interdisciplinary Studies, Khon Kaen University, Nong Khai Campus, Nong Khai, 43000, Thailand*
[2] *Department of Microbiology, Faculty of Science, Chulalongkorn University, Bangkok, 10330, Thailand*
[3] *National Nanotechnology Centre (NANOTEC), National Science and Technology Development Agency, Pathum Thani, Bangkok, 12120, Thailand*
[4] *Department of Genetics, Faculty of Science, Kasetsart University, Bangkok, 10900, Thailand*
[5] *The International Undergraduate Program in Bioscience and Technology, Faculty of Science, Kasetsart University, Bangkok, 10900, Thailand*
[6] *Program in Science Technology and Business Enterprise, Faculty of Interdisciplinary Studies, Khon Kaen University, Nong Khai Campus, Nong Khai, 43000, Thailand*
[7] *Department of Chemical Science, Faculty of Science, Universiti Tunku Abdul Rahman, Kampar, 31900, Malaysia*

***Corresponding author e-mail**: kitiwi@kku.ac.th

Received date:
29 February 2024
Revised date
2 April 2024
Accepted date:
23 May 2024

Keywords:
Zinc oxide nanoparticles;
Biosynthesis process;
Antimicrobial activity;
Dye removal;
Water hyacinth extracts

Abstract

In nanobiotechnology, synthesizing metal nanoparticles (NPs) using plant extracts has recently been increasing because of eco-friendly and low-cost methods. For this work, zinc oxide nanoparticles (ZnO NPs) have been synthesized by biosynthesis process using water hyacinth extracts (WHE). The water hyacinth (WH) was chosen because the WH is fast-growing and the most toxic aquatic plant in the world. Therefore, this work aims to apply these WHE to be a precursor in the biosynthesis of ZnO NPs (ZnO_{Bio}-NPs) based on the research of a sustainable environment. The ZnO NPs synthesized by the WHE were investigated for their antibacterial and photocatalytic activities. An UV-Vis spectrum showed a specific absorbance peak around 362 nm with an average band gap of 3.22 eV. As the result, TEM analysis revealed a triangle structure with an average size of about 64.05 nm. The peaks of XRD analysis show a hexagonal wurtzite structure. The ZnO NPs synthesized by the WHE showed higher antibacterial activity against *S. aureus* better than *E. coli*. It is interesting to note that the ZnO_{Bio}-NPs synthesized from the WHE can have an anti *P. acnes* (JB7) with a minimum inhibitory concentration (MIC) and a minimum bactericidal concentration (MBC) equal to 50 $\mu g \cdot mL^{-1}$ and 200 $\mu g \cdot mL^{-1}$, respectively. In addition, the ZnO_{Bio}-NPs also can effectively remove more than 90% of the malachite green within 180 minutes with extremely high reuse.

1. Introduction

Nanotechnology has played an important role in various fields such as catalysis, pharmaceutics, cosmetics, and environmental applications, etc. [1]. Zinc oxide nanoparticles (ZnO NPs) have been paid attention in past decades due to a unique character that can be applied in many industries [2]. Various approaches are used for ZnO NPs syntheses, including chemical and physical methods. However, these methods are not eco-friendly because of using toxic agents [3]. Therefore, green synthesis or biosynthesis is an alternative and low-cost method due to reducing hazardous processes compared to physical and chemical synthesis methods [4]. Among green processes, plant extract-mediated synthesis of ZnO can be produced on a large scale and without additional impurities. ZnO NPs are synthesized by plant extracts that can provide a variety of properties such as antimicrobial activity, and catalytic and optical properties [5].

Water hyacinth is fast growing and free-floating aquatic weed which is the most toxic aquatic plant in the world because it can change the chemical and physical structure of aquatic environments. In general, the water hyacinth is unwanted and needs to be removed from the river because of the above reasons. However, the water hyacinth can be used as the mediator because it has bioactive compounds (alkaloids, terpenoids, steroids, phenol, glycoside, and flavonoids) that can stabilize the nanoparticle formation [6,7]. Thus, the water hyacinth could give a potential application in the synthesis of ZnO NPs based on sustainable development goals (SDGs).

There are many reports on the properties of ZnO NPs synthesized from water hyacinths. Application for growth and seed production [8],

antibacterial on plant pathogenic bacteria [9], and nano-fertilizer [10]. For this work, we aim to synthesize the ZnO NPs from water hyacinth to investigate the antibacterial activity and the properties of cationic and anionic dye removal.

2. Experimental

2.1 Materials

Zinc acetate dihydrate ($Zn(CH_3COO)_2{\cdot}2H_2O$) (Kemaus, Australia), sodium hydroxide (AR grade), ethanol (Liquor distillery organization, Thailand), nutrient agar and nutrient broth (Himdia, India), 2,3,5-Triphenyltetrazolium chloride (TTC) (DC Fine chemicals,Spain), 1,1-diphenyl-2-picrylhydrazyl (DPPH) (Sigma-Aldrich, Germany), indigo dye (LOBA Chemie, India), malachite green dye (LOBA Chemie, India)

2.2 Methods

2.2.1 Preparation of water hyacinth extracts

Fresh water hyacinth (collected from Udon Thani, Thailand) was cleaned with tap water, and distilled water was rinsed in the last step. The cleaned water hyacinth was dried in a hot air oven at 60°C for 48 h and finely ground using a grinder. Next, 5 g of the dried powder were extracted in 200 mL of deionized water at 70°C for 30 min. Finally, the aqueous extracts were filtered using filter paper (Whatman No. 1) and then stored at 4°C for further use.

2.2.2 Biosynthesis of ZnO NPs using water hyacinth extracts

To synthesize ZnO NPs, 0.1 M of zinc acetate dihydrate was stirred with 2 mL of water hyacinth extracts for 10 min. Next, the mixture was adjusted to pH 12 with 2 M sodium hydroxide solution and stirred continuously at different temperatures for 1 h to find the optimum condition for the synthesis of ZnO NPs. Subsequently, the white precipitate was suspended and separated by centrifugation for 15 min at 12,000 rpm. The obtained precipitate was rinsed with deionized water, followed by ethanol. Finally, the precipitate was dried in the hot air oven at 80°C for 24 h. All steps of synthesis are presented in Figure 1.

2.2.3 Characterization of biosynthesized ZnO NPs

The suspended ZnO NPs in deionized water and water hyacinth extracts were investigated for absorption spectra between 300 nm and 600 nm using UV-Vis spectrophotometer. The band gaps were calculated based on extrapolating the linear component using the Tauc's plot [11,12]. To identify the functional groups, the water hyacinth extract and synthesized ZnO NPs were analyzed in the range of 4,000 cm^{-1} to 500 cm^{-1} using Fourier-transform infrared (FTIR) analysis. The crystalline structure of ZnO NPs was determined by using X-ray diffraction (XRD). The energy dispersive X-ray (EDX) is the technique to analyze the elements of the ZnO NPs. The shape and size of ZnO NPs were analyzed by using transmission electron microscope (TEM) technique.

2.2.4 Evaluation of antioxidant activity by DPPH method

The free radical scavenging activity (SC) of the samples (water hyacinth extracts and ZnO_{Bio}-NPs) was tested by 1,1-diphenyl-2-picrylhydrazyl (DPPH) based on the method of Chen *et al.* [13] with some modifications. The 0.1 mM solution of DPPH in 99.9% ethanol was prepared freshly before UV-Vis measurement. The concentration of the samples was prepared in the range of 500 $mg{\cdot}mL^{-1}$ to 3.906 $mg{\cdot}mL^{-1}$ and 500 $\mu g{\cdot}mL^{-1}$ to 3.906 $\mu g{\cdot}mL^{-1}$ for water hyacinth extracts and ZnO_{Bio}-NPs solutions, respectively, using a serial dilution. Next, 0.1 mL of sample was added into 2.9 mL of the prepared DPPH with shaking vigorously for 30 min in the dark. Then, the absorbance of obtained mixtures was measured at 517 nm by UV-Vis spectrophotometer. The ethanolic DPPH solution without the samples was used as a control. Each absorbance was converted into percentage SC (*%SC*) using Equation (1). The definitions of A_C and A_S are the absorbance for the control and the sample, respectively. All tests were performed in triplicate.

$$\% SC = \left(\frac{A_C - A_S}{A_C}\right) * 100 \quad (1)$$

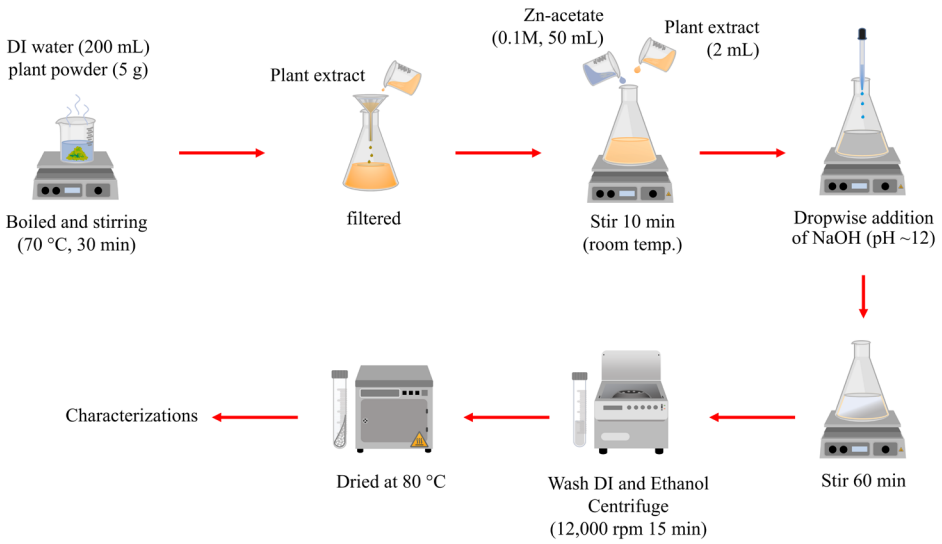

Figure 1. Illustration of biosynthesis of ZnO NPs by water hyacinth extracts.

2.2.5 Antimicrobial activity

In the present study, antimicrobial activity of ZnO_{Bio}-NPs was tested against Gram-negative bacterium *Escherichia coli* and Gram-positive bacteria *Staphylococcus aureus* [14] and *Propionibacterium acnes* (JB7).

2.2.5.1 Antimicrobial activity against Escherichia coli and Staphylococcus aureus

Determination of the minimum inhibitory concentration (MIC) and minimum bactericidal concentration (MBC) of the ZnO_{Bio}-NPs was performed by broth micro-dilution method using 2,3,5-triphenyl tetrazolium chloride (TTC) assay [9]. Concentrations of the ZnO_{Bio}-NPs in nutrient broth (NB) were prepared in the range of 0.039 mg·mL^{-1} to 5.00 mg·mL^{-1}. Each concentration of tested suspension was mixed with the bacterial culture (0.5 McFarland standard). The mixtures were incubated at 37°C for 24 h. before adding the TTC reagent (20 mg·mL^{-1}) and further incubated at 37°C for 3 h. The MBC was assessed by re-culturing 10 µL of the lowest concentration that bacterial growth was not observed from the MIC assay onto the nutrient agar (NA) plate by drop plate and incubated at 37°C for 24 h. All experiments were performed in triplicate.

2.2.5.2 Anti-Propionibacterium acnes activity

The *P. acnes* strain JB7 was cultured in BHIA broth and incubated at 37°C for 48 h. in an anaerobic condition. The 100 µL bacterial culture was inoculated into each well of a 96-well microplate. The MIC was determined in the ranges of 400 µg·mL^{-1} to 1.56 µg·mL^{-1} for ZnO_{Bio}-NPs, and Erythromycin (positive control). The MBC was assessed by subculturing 10 µL bacterial culture from 96-well plate and dropped onto BHIA agar plates and incubated at 37°C for 96 h. under anaerobic conditions.

2.2.6 Dye removal

The dye degradation activity of ZnO_{Bio}-NPs was assessed by degradation of cationic dye (Malachite Green) and anionic dye (Indigo) in the presence of UV-sunlight. To initiate photocatalytic degradation, 25 mg of ZnO_{Bio}-NPs were first added into 50 mL of dye solution, at a concentration of 20 ppm (20 mg·L^{-1}) and a neutral pH. Next, the mixture solution was sonicated for about 15 min. Then the mixture was shaken for 30 min in the dark condition to reach adsorption-desorption equilibrium. After that, the mixture was reacted under UV-sunlight for 10, 20, 30, 60, 90, 120, and 180 min. After that, 2 mL of the irradiated solution was taken out, centrifuged and its absorbance was measured using a UV-Vis spectrophotometer (300 nm to 800 nm). Here without ZnO_{Bio}-NPs in dye solution was taken as a control dye. The degradation efficiency of the dye was calculated using Equation (2).

$$\% \, Degradation = \left(\frac{A_i - A_t}{A_i}\right) \times 100 \qquad (2)$$

A_i is the absorbance of dye without ZnO_{Bio}-NPs (control) and A_t is the absorbance of dye with ZnO_{Bio}-NPs reaction mixture at time t [15,16]. In addition, the solution conductivity was investigated to present the decrease of organic compounds based on dye degradation. The reusability was reported for four cycles.

3. Results and discussion

3.1 Characterization of ZnO_{Bio}-NPs synthesized by using water hyacinth extract

3.1.1 FTIR analysis

To identify the functional groups of the water hyacinth extracts and the ZnO_{Bio}-NPs, FTIR spectroscopy was applied and shown in Figure 2. The broad peaks of the plant extracts and the ZnO_{Bio}-NPs at 3240 cm^{-1} indicate the existence of O–H stretching of complexes. For the plant extracts, the peaks at 1595 cm^{-1} show carbonyl stretching (C–O) and the O–H group that agrees with the previous studies [9]. This peak also suggested that the carbonyl group is contained in the polysaccharide ring of cellulose which was confirmed at the wavenumber ~1325 cm^{-1} as Pratama *et al*. [17]. In addition, the wavenumber ~1058 cm^{-1} shows the C–O–C in the pyranose ring as shown in the previous studies [17]. For the ZnO_{Bio}-NPs, the smaller band vibration ~880 cm^{-1} was referred from C-H stretching (alkane) as shown in Figure 2(b-d). This indicates the successful synthesis of Zn-O symmetrical bending of wurtzite ZnO. For the wavenumber between ~440 cm^{-1} to ~500 cm^{-1} in Figure 2(b-d), these wavenumbers the different sizes of ZnO nanoparticles [18].

3.1.2 Morphological analysis

The morphological study of the ZnO_{Bio}-NPs was carried out by TEM. The shape of the ZnO_{Bio}-NPs synthesized at 70°C is mainly a triangle structure with the average size about 64.05 nm. The EDX analysis presents the atomic weight of oxygen and zinc which are 52.81% and 47.19%, respectively, show in Figure 3(d).

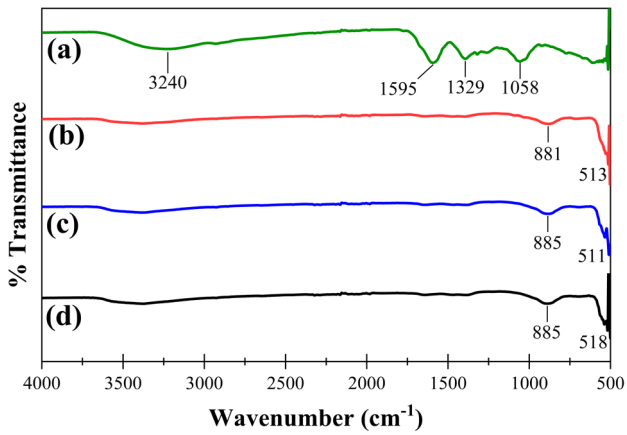

Figure 2. FTIR analysis of (a) water hyacinth and ZnO_{Bio}-NPs at (b) 30°C, (c) 50°C, and (d) 70°C, respectively.

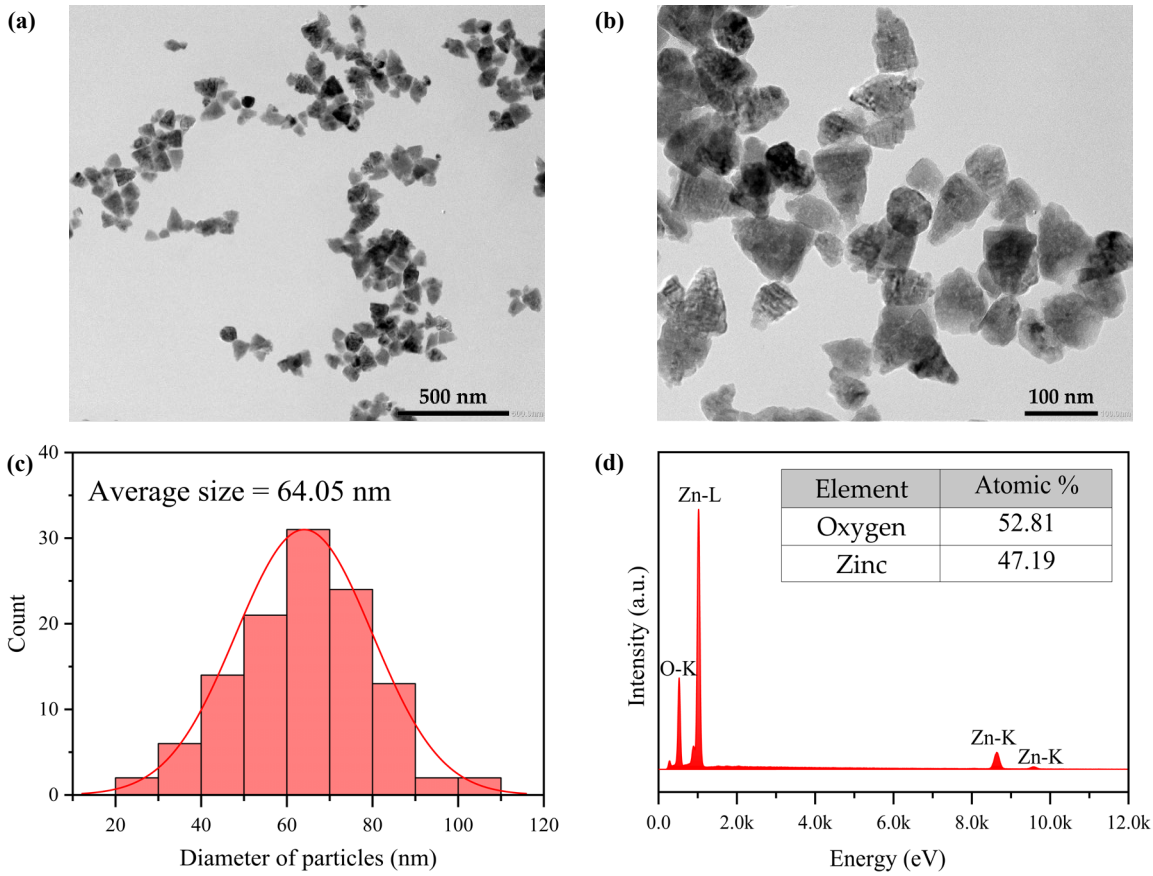

Figure 3. TEM micrograph and size distribution and EDX of zinc oxide nanoparticles synthesized at 70°C, (a-b) TEM, (c) size distribution, and (d) elemental composition.

3.1.3 X-ray diffraction analysis (XRD)

Figures 4(a-c) show the X-ray diffraction pattern of the ZnO_{Bio}-NPs synthesized at different temperatures (30°C, 50°C, 70°C). These peaks are potentially attributed to the crystallographic planes (100), (002), (101), (102), and (110) of the hexagonal wurtzite structure (JCPDF file no. 00-036-1451) of ZnO NPs as the previously reported [19].

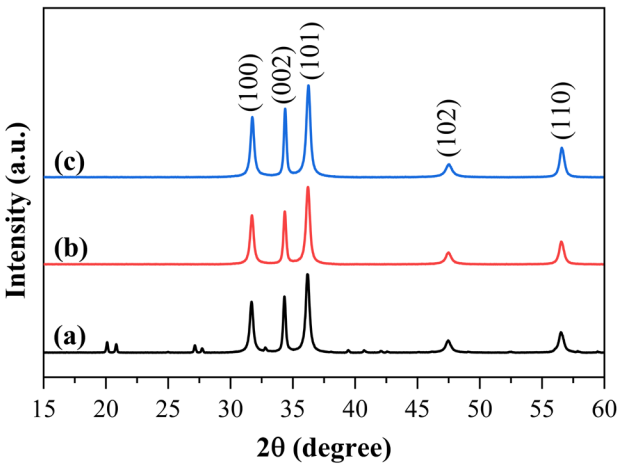

Figure 4. XRD pattern of zinc oxide nanoparticles, (a) 30°C, (b) 50°C, and (c) 70°C.

3.1.4 UV-vis absorption characteristics

The plot of the UV spectra (Figure 5) confirms the formation of ZnO_{Bio}-NPs with the wavelength of 362 nm [20]. The band gap of the ZnO_{Bio}-NPs was performed by using UV-visible spectroscopy. As the Figure 5, the band gap of the ZnO_{Bio}-NPs was 3.22 eV which can explain whether the ZnO_{Bio}-NPs can be used in a photocatalytic reaction. According to the reports [21], it explained that the small band gap is easily excited from the valence to the conduction band.

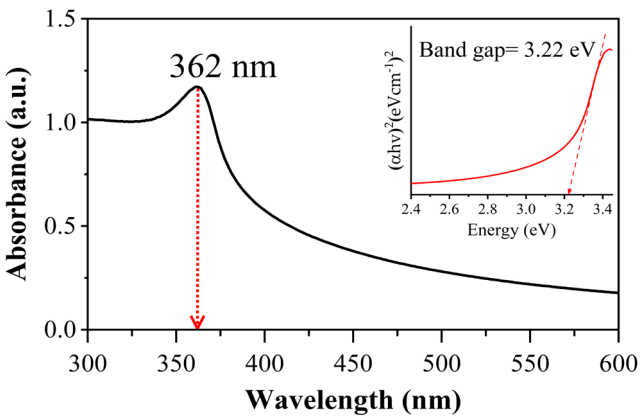

Figure 5. UV-Vis spectra and band gap energy of green synthesized ZnO NPs; absorption spectrum synthesized and band gap energy of synthesis at 70°C.

3.2 Antioxidant activity using DPPH assay

The DPPH scavenging assay was used to evaluate the free radical scavenging activity of the ZnO_{Bio}-NPs and water hyacinth extracts. The results show that there is a large number of phytochemicals in the plant extracts which leads to a higher *%SC* as shown in Figure 6(a). This supports the fact that the phytochemicals groups can be a capping agent for the biosynthesis of ZnO_{Bio}-NPs using the plant extracts [22]. When the ZnO_{Bio}-NPs appeared, the phytochemical groups decreased as shown in the functional groups shown in FTIR analysis. As illustrated in Figure 6(b), it is clearly shown that the *%SC* of Ascorbic acid, a standard substance, is higher than the *%SC* of the ZnO_{Bio}-NPs. Despite an increase in the concentration of ZnO_{Bio}-NPs, the antioxidant activity of ZnO_{Bio}-NPs does not substantially increase. This finding is consistent with the previous studies [23], which found that the antioxidant efficacy of the ZnO_{Bio}-NPs is reduced because of the lower solubility of the ZnO_{Bio}-NPs.

3.3 Antimicrobial activity

The ZnO_{Bio}-NPs against *S. aureus* and *E. coli* as shown in MIC and MBC values (Table 1). The MIC value of the ZnO_{Bio}-NPs against *E. coli* was measured at 312.50 $\mu g \cdot mL^{-1}$ and for *S. aureus* was at 156.25 $\mu g \cdot mL^{-1}$. The MBC of ZnO_{Bio}-NPs against *E. coli* was 5,000 $\mu g \cdot mL^{-1}$ and for *S. aureus* was 2,500 $\mu g \cdot mL^{-1}$. These results are supported by the previous studies [24,25] that the ZnO_{Bio}-NPs can invade the peptidoglycan layer of the *S. aureus.* While it is difficult to attack lipopolysaccharides of the *E. coli.* In addition, the ZnO_{Bio}-NPs also against *P. acnes* were 50 and 200 $\mu g \cdot mL^{-1}$, respectively. Although, the antibacterial activities of the ZnO_{Bio}-NPs are lower than the standard substances (Chloramphenicol and Erythromycin), these results show that the biosynthesized ZnO NPs can be used as an antibacterial agent very well.

3.4 Dye removal activity

As the photocatalytic results, it appears that the ZnO_{Bio}-NPs from the water hyacinth extracts can remove the malachite green (cationic dye) and indigo (anionic dye) efficiently. It is clearly to see that the absorbance of both dyes without the ZnO_{Bio}-NPs slightly decreased compared with time as seen in the plots in Figure 7(a) and Figure 8(a). Therefore, it implies that the degradation of both dyes is decreased by the effect of adding the ZnO_{Bio}-NPs as catalysts. It found that the malachite green was degraded in the first ten minutes with about 73.32% degradation and reached about 95.15% degradation within 180 min (Figure 7). For the indigo degradation (Figure 8), it was found that the degradation gradually increased from 20 min (25.98% degradation) to 180 min (83.17% degradation).

Degradation studies were carried out four times with the same ZnO_{Bio}-NPs as described in the previous study [26] to investigate the reusability of the ZnO_{Bio}-NPs. The results are presented in Figure 9. It appears that the ZnO_{Bio}-NPs can be reused to remove malachite green more efficiently than the indigo because the percent of degradation efficiency slightly changes from the first (95.15%) to the fourth (94.74%) time for malachite green. While, the percent of degradation efficiency of indigo drops by almost 10% from the first (83.17%) to the fourth (74.25%) time. These results show that the ZnO_{Bio}-NPs can be reused extremely high for removing malachite green.

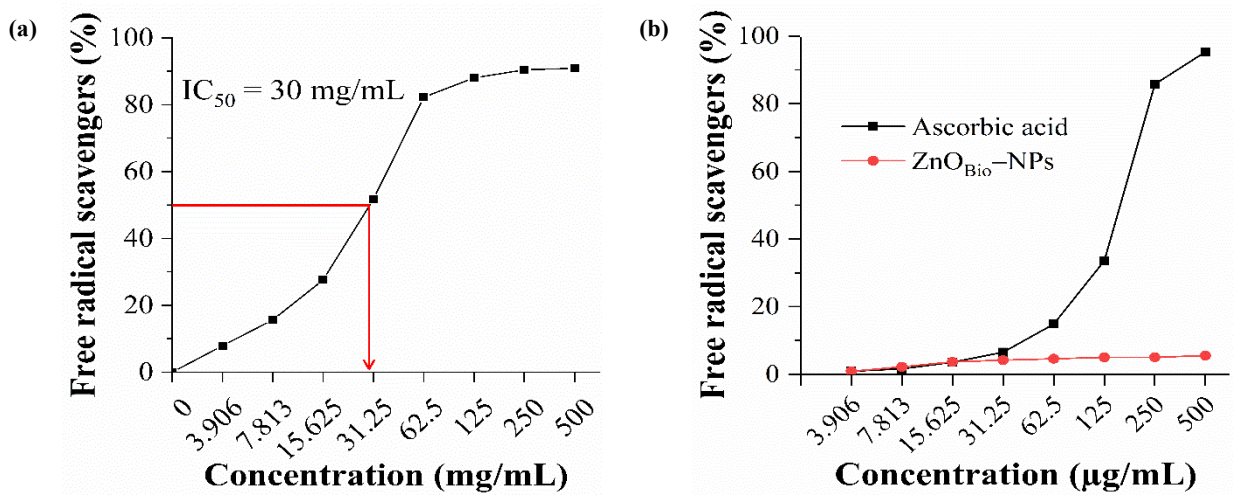

Figure 6. % Scavenging of (a) plant extract and (b) ZnO_{Bio}-NPs and ascorbic acid evaluated by DPPH assay.

Table 1. MIC value and MBC value of ZnO_{Bio}-NPs.

Sample	Bacterial species					
	E. coli		*S. aureus*		*P. acnes*	
	MIC*	MBC*	MIC*	MBC*	MIC*	MBC*
Chloramphenicol	3.125	400	12.5	400	-	-
Erythromycin	-	-	-	-	1.56	1.56
ZnO_{Bio}-NPs	312.50	5,000	156.25	2,500	50	200

* $\mu g \cdot mL^{-1}$ of concentration

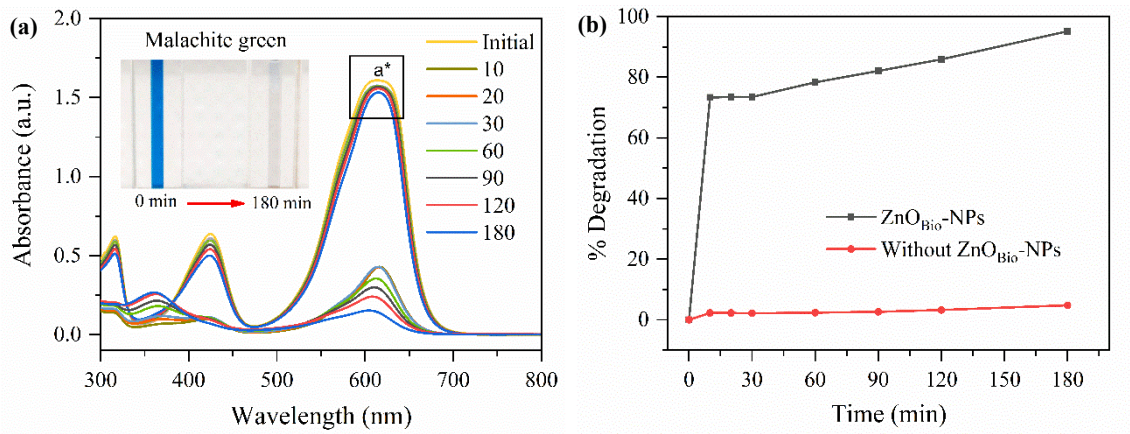

Figure 7. Photocatalytic activity of ZnO$_{Bio}$-NPs in degradation of malachite green: (a) UV-Vis spectra of malachite green dye with respect to irradiation (a* is the spectra of malachite green without ZnO$_{Bio}$-NPs at interval time) (b) % degradation of dye with irradiation time.

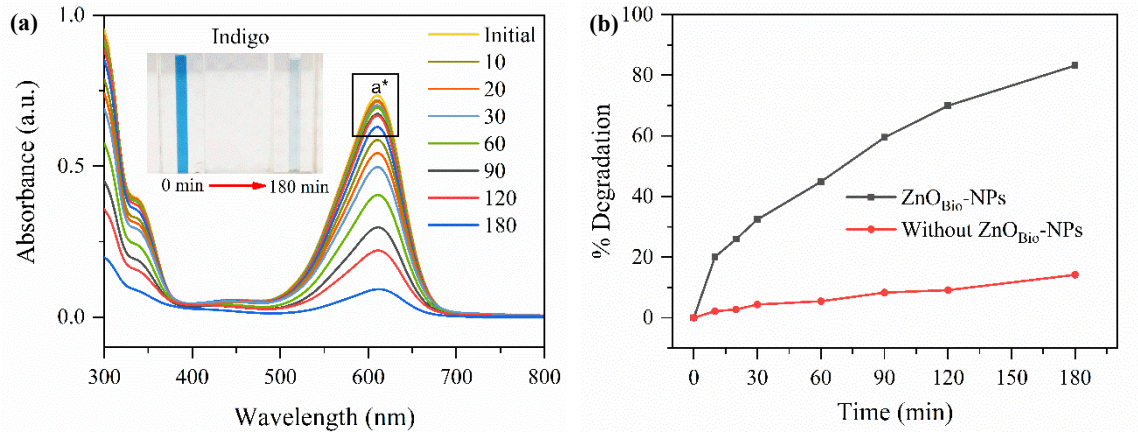

Figure 8. Photocatalytic activity of ZnO$_{Bio}$-NPs in degradation of indigo: (a) UV-Vis spectra of indigo dye with respect to irradiation (a* is the spectra of malachite green without ZnO$_{Bio}$-NPs at interval time) (b) % degradation of dye with irradiation time.

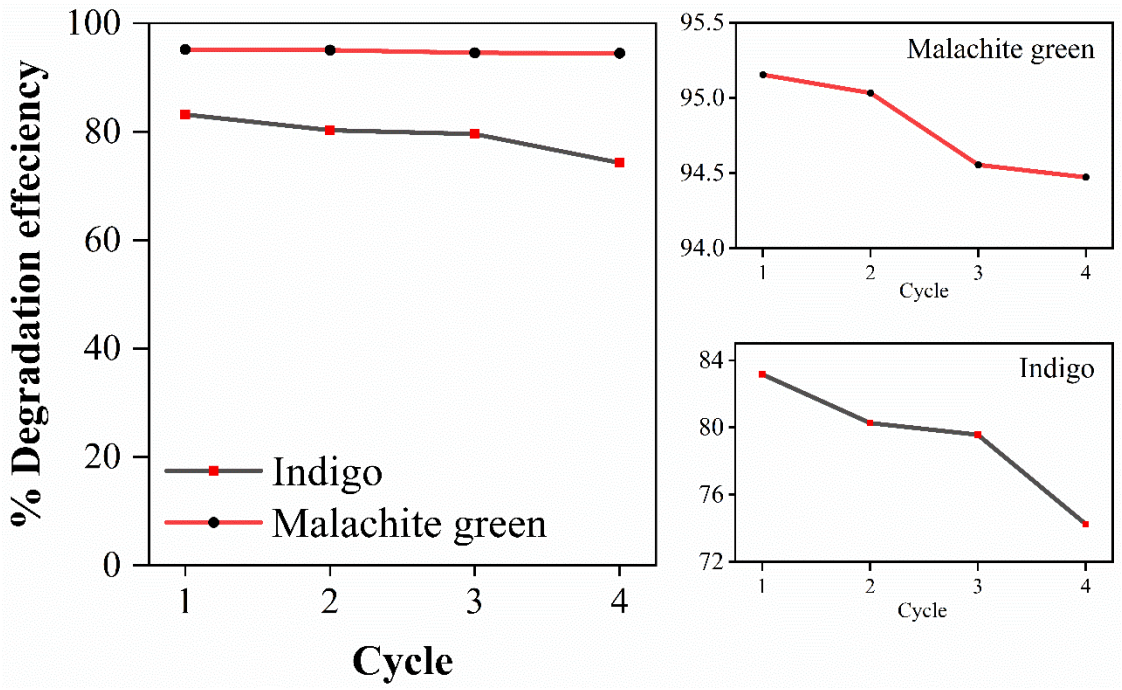

Figure 9. Recoverability and stability of ZnO$_{Bio}$-NPs photocatalyst in four successive cycles

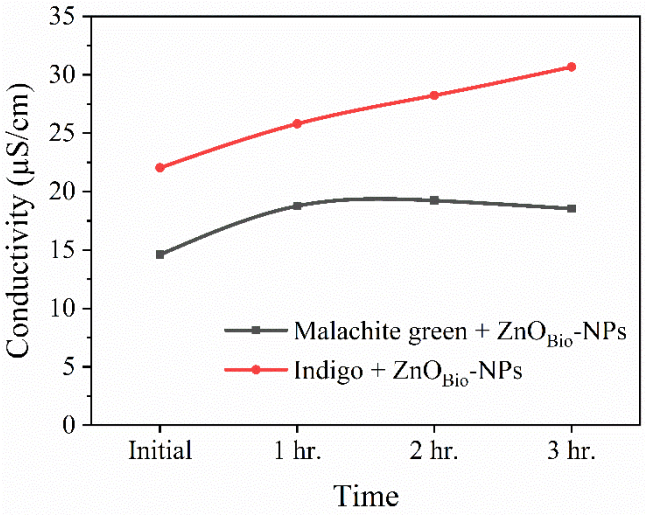

Figure 10. The solution conductivity of malachite green (black line) and indigo (red line) versus times.

In addition, our work also shows the relationship between conductivity and the percent degradation efficiency. This relationship can reflect the removal of the total organic compounds (TOCs) because the higher conductivity shows the lower amount of organic compounds (higher amount of inorganic compounds). In Figure 10, the results show that the solution conductivity is higher according to time increases from 1 h to 3 h for both dyes. Therefore, this implies that the percent degradation efficiency of dye is related to the decrease of the organic compounds that are the source of the higher trend of conductivity.

4. Conclusions

This work is focused on the synthesis of the ZnO_{Bio}-NPs using the WTE to investigate the antibacterial and photocatalytic. The XRD and TEM analysis show the crystalline structure and the size of the obtained ZnO NPs. The EDX shows the atomic weight of oxygen and zinc which are 52.81% and 47.19%, respectively. The ZnO_{Bio}-NPs shows the antibacterial activity for *S. aureus*, *E. coli*, and *P. acnes.* In addition, the ZnO_{Bio}-NPs were also effective in the degradation of malachite green and indigo. Our work shows the ZnO_{Bio}-NPs can be reused extremely high for removing malachite green. Moreover, the higher conductivity reflects the lower amount of organic compounds which is consistent with dye degradation efficiency. This work can show the ability of ZnO_{Bio}-NPs from using the WTE as a part of the synthesis to be an alternative material for cosmetic, medicine, and degradation dyes applications.

Acknowledgements

P. S. and K. W. would like to thank the research and graduate studies (RP64-4-002), Khon Kaen University for their financial support. P. S. and K. W. also would like to thank Asst. Prof. Dr. Supachai Sompech for muffle furnace support.

References

[1] A. M. Salih, F. Al-Qurainy, S. Khan, M. Tarroum, M. Nadeem, H. O. Shaikhaldein, A. R. Z. Gaafar, and N. S. Alfarraj, "Biosynthesis of zinc oxide nanoparticles using Phoenix dactylifera and their effect on biomass and phytochemical compounds in Juniperus procera," *Scientific Reports*, vol. 11, p. 19136, 2021.

[2] H. Mohd Yusof, N. A. Abdul Rahman, R. Mohamad, U. H. Zaidan, and A. A. Samsudin, "Biosynthesis of zinc oxide nanoparticles by cell-biomass and supernatant of Lactobacillus plantarum TA4 and its antibacterial and biocompatibility properties," *Scientific Reports*, vol. 10, no. 1, p. 19996, 2020.

[3] A. M. Awwad, N. M. Salem, and A. O. Abdeen, "Green synthesis of silver nanoparticles using carob leaf extract and its antibacterial activity," *International Journal of Industrial Chemistry*, vol. 4, no. 1, pp. 29, 2013.

[4] S. Ahmed, M. Ahmad, B. L. Swami, and S. Ikram, "A review on plants extract mediated synthesis of silver nanoparticles for antimicrobial applications: A green expertise*," Journal of Advanced Research*, vol. 7, no. 1, pp. 17-28, 2016.

[5] S. T. Khan, J. Musarrat, and A. A. Al-Khedhairy, "Countering drug resistance, infectious diseases, and sepsis using metal and metal oxides nanoparticles: current status," *Colloids and Surfaces. B, Biointerfaces*, ol. 146, pp. 70-83, 2016.

[6] G. Jagathesan and P. Rajiv, "Biosynthesis and characterization of iron oxide nanoparticles using Eichhornia crassipes leaf extract and assessing their antibacterial activity," *Biocatalysis and Agricultural Biotechnology*, vol. 13, pp. 90-94, 2018.

[7] O. A. Zelekew, S. G. Aragaw, F. K. Sabir, D. M. Andoshe, A. D. Duma, K. Dong-Hau, X. Chen, and G. K. Devulapalli, "Green synthesis of CO-doped ZnO via the accumulation of cobalt ion onto Eichhornia crassipes plant tissue and the photocatalytic degradation efficiency under visible light," *Materials Research Express*, vol. 8, p. 025010, 2021.

[8] P. Rajiv, P. Vanathi, and A. Thangamani, "An investigation of phytotoxicity using Eichhornia mediated zinc oxide nanoparticles on Helianthus annuus," *Biocatalysis and Agricultural Biotechnology*, vol. 16, pp. 419-424, 2018.

[9] T. Jaithon, J. Ruangtong, J. T-Thienprasert, and P. N. T-Thienprasert, "Effects of waste-derived ZnO nanoparticles against growth of plant pathogenic bacteria and epidermoid carcinoma cells," *Crystals*, vol. 12, no. 6, p. 779, 2022.

[10] M. Kalaivani, and S. Ravi, "Green synthesis of ZnO NPs and CdO-ZnO nanocomposites using aqueous extract of water hyacinth (Eichhornia crassipes) characterization, structural and nano-fertilizer using application," *Indian Journal of Science and Technology,* vol. 16, no. 25, pp. 1918-1926, 2023.

[11] J. Tauc, R. Grigorovici, and A. Vancu, "Optical properties and electronic structure of amorphous germanium," *Physica Status Solidi (B)*, vol. 15, no. 2, pp. 627-637, 1966.

[12] M. Kalaivani and S. Ravi, "Green synthesis of ZnO NPs and CdO-ZnO nanocomposites using aqueous extract of water

hyacinth (Eichhornia crassipes) characterization, structural and nano-fertilizer using application," *Indian Journal of Science and Technology*, vol. 16, no. 25, pp. 1918-1926, 2023.

[13] Y. Chen, M. Y. Xie, S. P. Nie, C. Li, and Y. X. Wang, "Purification, composition analysis and antioxidant activity of a polysaccharide from the fruiting bodies of Ganoderma atrum," *Food Chemistry*, vol. 107, no. 1, pp. 231-241, 2008.

14] S. Audtarat, P. Hongsachart, T. Dasri, S. Chio-Srichan, S. Soontaranon, W. Wongsinlatam, S. Sompech, "Green synthesis of silver nanoparticles loaded into bacterial cellulose for anti-microbial application," *Nanocomposites*, vol. 8, no. 1, pp.34-46, 2022.

[15] O. K. Hee, E. J. Rupa, G. Anandapadmanaban, M. Chokkalingam, J. F. Li, J. Markus, V. Soshnikova, Z. E. J. Perez, D. C. Yang, "Cationic and anionic dye degradation activity of zinc oxide nanoparticles from Hippophae rhamnoides leaves as potential water treatment resource," *Optik*, vol. 181, pp. 1091-1098, 2019.

[16] J. K. Park, E. J. Rupa, M. H. Arif, J. F. Li, G. Anandapadmanaban, J. P. Kang, M. Kim, J. C. Ahn, R. Akter, D. C. Yang, and S. C. Kang, "Synthesis of zinc oxide nanoparticles from Gynostemma pentaphyllum extracts and assessment of photocatalytic properties through malachite green dye decolorization under UV illumination-A Green Approach," *Optik*, Vol. 239, p. 166249, 2021.

[17] J. H. Pratama, A. Amalia, R. L. Rohmah, and T. E Saraswati, "The extraction of cellulose powder of water hyacinth (Eichhornia crassipes) as reinforcing agents in bioplastic," *AIP Conference Proceedings*, vol. 2219, no. 1, p. 100003, 2020.

[18] N. S. Ferreira, J. M. Sasaki, R. S. Silva, J. M. Attah-Baah, and M. A. Macêdo, "Visible-light-responsive photocatalytic activity significantly enhanced by active [VZn + V+O] defects in self-assembled ZnO nanoparticles," Inorganic Chemistry, vol. 60, no. 7, pp. 4475-4496, 2021.

[19] S. Faisal, H. Jan, S. A. Shah, S. Shah, A. Khan, M. T. Akbar, M. Rizwan, F. Jan, Wajidullah; N. Akhtar, A. Khattak, and S. Syed, "Green synthesis of zinc oxide (ZnO) nanoparticles using aqueous fruit extracts of Myristica fragrans: their characterizations and biological and environmental applications," *ACS Omega.* vol. 6, no. 14, pp. 9709-9722, 2021.

[20] F. A. M. Alahdal, M. T. A. Qashqoosh, Y. K. Manea, M. A. S. Salem, A. M. T. Khan, and S. Naqvi, "Eco-friendly synthesis of zinc oxide nanoparticles as nanosensor, nanocatalyst and antioxidant agent using leaf extract of P. austroarabica," *OpenNano*, vol. 8, p. 100067, 2022.

[21] L. Fu and Z. Fu, "Plectranthus amboinicus leaf extract–assisted biosynthesis of ZnO nanoparticles and their photocatalytic activity." *Ceramics International*, vol. 41, no. 2, pp. 2492-2496, 2015.

[22] A. Happy, M. Soumya, S. Venkat Kumar, S. Rajeshkumar, N. D. Sheba Rani, T. Lakshmi, and V. Deepak Nallaswamy, "Phyto-assisted synthesis of zinc oxide nanoparticles using Cassia alata and its antibacterial activity against Escherichia coli," *Biochemistry and Biophysics Reports*, vol. 17, pp. 208-211, 2019.

[23] B. Kumar, K. Smita, R. Seqqat, K. Benalcazar, M. Grijalva, and L. Cumbal, "In vitro evaluation of silver nanoparticles cytotoxicity on Hepatic cancer (Hep-G2) cell line and their antioxidant activity: Green approach for fabrication and application," *Journal of Photochemistry and Photobiology. B, Biology*, vol. 159, pp. 8-13, 2016.

[24] B. L. Silva, M. P. Abuçafy, E. B. Manaia, J. A. O. Junior, B. G. Chiari-Andréo, R. C. L. R. Pietro, and L. A. Chiavacci, "Relationship between structure and antimicrobial activity of zinc oxide nanoparticles: an overview." *International Journal of Nanomedicine*, vol. 14, pp. 9395-9410, 2019.

[25] R. Hamed, R. Z. Obeid, and R. Abu-Huwaij, "Plant mediated-green synthesis of zinc oxide nanoparticles: An insight into biomedical applications," *Nanotechnology Reviews*, vol. 12, no. 1, p. 20230112, 2023.

[26] R. Kitture, S. J. Koppikar, R. Kaul-Ghanekar, S. N. Kale, "Catalyst efficiency, photostability and reusability study of ZnO nanoparticles in visible light for dye degradation," *Journal of Physics and Chemistry of Solids*, vol. 72, no. 1, pp. 60-66, 2011.